Separation Science and Technology
Publication details, including instructions for authors and subscription information:
http://www.informaworld.com/smpp/title~content=t713708471

Exact Analysis of Field-Flow Fractionation

Sowmithri Krishnamurthy[ab]; R. Shanker Subramanian[a]
[a] CHEMICAL ENGINEERING DEPARTMENT, CLARKSON COLLEGE OF TECHNOLOGY, POTSDAM, NEW YORK [b] Department of Chemical and Petroleum Engineering, University of Pittsburgh, Pittsburgh, Pennsylvania

To cite this Article Krishnamurthy, Sowmithri and Subramanian, R. Shanker(1977) 'Exact Analysis of Field-Flow Fractionation', Separation Science and Technology, 12: 4, 347 — 379
To link to this Article: DOI: 10.1080/00372367708058083
URL: http://dx.doi.org/10.1080/00372367708058083

SEPARATION SCIENCE, 12(4), pp. 347–379, 1977

Exact Analysis of Field-Flow Fractionation

SOWMITHRI KRISHNAMURTHY*
and R. SHANKAR SUBRAMANIAN†

CHEMICAL ENGINEERING DEPARTMENT
CLARKSON COLLEGE OF TECHNOLOGY
POTSDAM, NEW YORK 13676

Abstract

A rigorous convective diffusion theory is formulated for the predictive modeling of field-flow fractionation (FFF) columns used for the separation of colloidal mixtures. The theory is developed for simulating the behavior of a colloid introduced into fluid in time-dependent flow in a parallel plate channel across which a transverse field is applied. The methodology of generalized dispersion theory is used to solve the model equations. The theoretical results show that the cross-sectional average concentration of the colloid satisfies a dispersion equation with time-dependent coefficients. The results of this work, in principle, are valid for all values of time since the introduction of the colloid. It is shown that these results asymptotically approach those of the nonequilibrium theory formulated by Giddings for large values of time.

Illustrative numerical results are obtained for the case of steady laminar flow and a uniform initial distribution. The behavior of the coefficients in the dispersion equation is explained on physical grounds. Of particular interest is the fact that at large values of the transverse Peclet number P, Taylor dispersion in the FFF column is very small. Under these conditions, axial molecular diffusion as well as Taylor dispersion in the connecting tubing could make a substantial contribution to the axial dispersion observed in practical FFF columns.

The theoretical predictions are compared with the experimental data of Caldwell et al. and Kesner et al. on electrical FFF columns. The comparisons

*Present address: Department of Chemical and Petroleum Engineering, University of Pittsburgh, Pittsburgh, Pennsylvania 15260.

†Formerly R. Sankarasubramanian.

indicate that the theory has potential in predicting the performance of such systems.

INTRODUCTION

Giddings (*1*) introduced the term "field-flow fractionation" (FFF) to describe a broad class of separation methods he and his co-workers have pioneered in the analysis of colloidal mixtures. The basic technique consists of introducing a colloidal mixture into fluid in laminar flow in a channel. As the sample is convected downstream, a transverse field (which, for instance, may be electrical, thermal, or gravitational) forces the different species to form different transverse distributions, the natures of which depend on the field strength and the properties of each specie. Since the velocity profile in the fluid is distributed, each specie will be convected at a characteristic velocity with a resulting separation at a downstream monitoring station. The actual application of the technique with various fields has been demonstrated in numerous articles by Giddings and co-workers (*2–10*). A similar concept also has been employed by Lee et al. (*11*) who used ultrafiltration in hollow fiber systems to achieve the desired transverse distributions; they termed their technique "single phase chromatography." Recently, using the concept of electrical FFF demonstrated by Caldwell et al. (*6*), Reis and Lightfoot (*12*) have achieved the separation of proteins in hollow fibers with transverse electric fields. They suggest the alternate name "electropolarization chromatography" to describe their method.

The technique of field flow fractionation is proving to be not only a powerful analytical device but also a highly useful method for the determination of important physical properties of colloids as illustrated by Giddings et al. (*9, 10, 13*).

A theoretical treatment of FFF was proposed by Giddings (*14*) in 1968 and elaborated on by Hovingh et al. (2), Myers et al. (*5*), and Giddings et al. (*15, 16*) in later years. Giddings's approach, referred to as "nonequilibrium theory" in view of its origin in chromatography [Giddings (*17*)], employs intuitive assumptions similar to those of Taylor (*18, 19*) who studied solute dispersion in a capillary in the absence of interphase transport or transverse fields. Taylor's results are valid asymptotically in the limit of large values of time since the introduction of solute into the flow, and it will be shown here that Giddings's results, similarly, enjoy asymptotic validity.

The Taylor dispersion problem has been solved exactly by Gill and Sankarasubramanian (*20, 21*) using generalized dispersion theory. These

investigators showed that the average concentration distribution in such problems satisfies a generalized dispersion equation with time-dependent coefficients. They also showed that this model asymptotically approaches the constant coefficient Taylor–Aris (*22*) dispersion model. It is the purpose of the present work to construct an exact mathematical description of unsteady convective diffusion in field flow fractionation columns using the tools of generalized dispersion theory. The theory will be used to identify the relevant dimensionless parameters of interest and indicate their influence on the behavior of FFF systems. The basic methodology will be illustrated for the parallel plate geometry employed by Giddings and co-workers but would be equally applicable to other geometries such as the circular hollow fiber systems employed by Lightfoot and co-workers.

ANALYSIS

The unsteady convective diffusion of a colloidal specie introduced into a fluid in time-variable laminar flow in a channel formed by two parallel plates will be analyzed. The plates are $2b$ units apart and are a units wide. The coordinate system is shown in Fig. 1. A transverse field is imposed in the y-direction, causing the colloid to migrate at a constant velocity v in that direction. If this field is electric, the plates forming the channel will actually be semipermeable membranes which will prevent the colloid from leaving the channel while still permitting ions to enter and leave freely. The electrodes would then be mounted in separate chambers on either side of the channel (*6*, *7*). It should be noted that thermal FFF does not fall in the same category as the others because the equivalent transverse migration velocity v is a strong function of transverse position. Therefore, the analysis will have to be modified appropriately in order to be applicable to TFFF.

In the theoretical treatment here, the unsteady convective diffusion of one colloidal specie is analyzed. To predict the concentration profiles of a multicomponent colloidal mixture, profiles of individual species may be

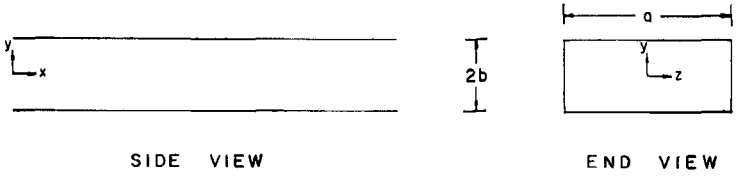

FIG. 1. Coordinate system.

obtained and superimposed if one makes the assumption that the different species do not interact with each other. In addition, the following simplifying assumptions are made about the system.

1. The aspect ratio of the system is assumed to be large; side wall effects will be ignored. Hence the velocity and concentration fields may be assumed to be independent of the z-coordinate.
2. The flow is fully developed and laminar. The time-variable axial velocity is described by $u = u(t, y)$; there are no velocity components in the y- and z-direction.
3. The walls of the system are impermeable to the colloidal particles.
4. Adsorption of the colloid on the channel walls is assumed to be negligible; this has been shown, in general, to be a good assumption by the experimental work of Lee et al. (*11*).
5. The solute concentration is sufficiently low; therefore free convection effects may be ignored.
6. In the case of electrical field-flow fractionation:
   a. The power dissipation in the channel is assumed to be negligible so that the free convection effects due to thermal gradients can be ignored.
   b. Electroosmotic effects will be ignored.

Under these conditions the local concentration of the colloid $c(t, x, y)$ will satisfy the following convective diffusion equation:

$$\frac{\partial c}{\partial t} + u\frac{\partial c}{\partial x} + v\frac{\partial c}{\partial y} = D\left[\frac{\partial^2 c}{\partial x^2} + \frac{\partial^2 c}{\partial y^2}\right] \tag{1}$$

The initial condition on c may be written as

$$c(0, x, y) = c_0 h_1(x) h_2(y) \tag{2a}$$

Here c_0 is a reference concentration which will subsequently be related to the total mass of the colloid introduced at the inlet.

Since the channel walls are impermeable to the colloid, and since there is no adsorption of the colloid on these walls, the flux of the colloid across either wall is zero and, therefore,

$$-D\frac{\partial c}{\partial y}(t, x, b) + vc(t, x, b) = 0 \tag{2b}$$

$$-D\frac{\partial c}{\partial y}(t, x, -b) + vc(t, x, -b) = 0 \tag{2c}$$

In view of the rather complex interactions between the colloidal particles adjacent to a boundary with that boundary, Eqs. (2b) and (2c) are, in a strict sense, only macroscopic approximations to reality. They may be shown to follow the assumptions of no colloid loss from the system and a constant v by suitable integration of Eq. (1).

Since the amount of colloid introduced is finite,

$$c(t, \infty, y) = 0 \tag{2d}$$

Equations (1) and (2) can be written in dimensionless form as

$$\frac{\partial \theta}{\partial \tau} + U(\tau, Y)\frac{\partial \theta}{\partial X} + \mathrm{P}\frac{\partial \theta}{\partial Y} = \left[\frac{1}{\mathrm{Pe}^2}\frac{\partial^2 \theta}{\partial X^2} + \frac{\partial^2 \theta}{\partial Y^2}\right] \tag{3}$$

with the conditions

$$\theta(0, X, Y) = H_1(X)H_2(Y) \tag{4a}$$

$$\frac{\partial \theta}{\partial Y}(\tau, X, 1) = \mathrm{P}\theta(\tau, X, 1) \tag{4b}$$

$$\frac{\partial \theta}{\partial Y}(\tau, X, -1) = \mathrm{P}\theta(\tau, X, -1) \tag{4c}$$

$$\theta(\tau, \infty, Y) = 0 \tag{4d}$$

where

$$\theta = c/c_0$$

$$U(\tau, Y) = u(t, y)/u_0$$

$$X = Dx/b^2u_0$$

$$Y = y/b$$

$$P = bv/D$$

$$\mathrm{Pe} = bu_0/D$$

$$\tau = Dt/b^2$$

$$H_1(X) = h_1(x)$$

$$H_2(Y) = h_2(y)$$

u_0 is a reference velocity, b is the half-width of the channel, and D is the diffusivity of the colloid.

Equations (3) and (4) can be solved by the generalized dispersion theory

developed by Gill and Sankarasubramanian (*20, 21*). Following their procedure, the solution for $\theta(\tau, X, Y)$ is written as

$$\theta(\tau, X, Y) = \sum_{k=0}^{\infty} f_k(\tau, Y) \frac{\partial^k \theta_m}{\partial X^k} \tag{5}$$

where the dimensionless area average concentration θ_m is given by

$$\theta_m(\tau, X) = \frac{1}{2} \int_{-1}^{+1} \theta(\tau, X, Y)\, dY \tag{6}$$

Integration of Eq. (3) with respect to Y from $Y = -1$ to $Y = +1$, followed by the use of Eqs. (4b) and (4c), leads to the generalized dispersion equation for $\theta_m(\tau, X)$:

$$\frac{\partial \theta_m}{\partial \tau} = \sum_{i=1}^{\infty} K_i(\tau) \frac{\partial^i \theta_m}{\partial X^i} \tag{7}$$

where

$$K_i(\tau) = \frac{\delta_{i2}}{\mathrm{Pe}^2} - \frac{1}{2} \int_{-1}^{+1} f_{i-1}(\tau, Y) U(\tau, Y)\, dY \qquad (i = 1, 2, 3, \ldots) \tag{8}$$

Equation (7) may be solved for $\theta_m(\tau, X)$ if the coefficients $K_i(\tau)$ are known. This requires a knowledge of the functions $f_k(\tau, Y)$. To find these, Eq. (5) representing the solution will be substituted in Eq. (3). After evaluating the mixed derivatives of the form $\partial^{k+1}\theta_m/\partial\tau\partial X^k$ in terms of $\partial^i \theta_m/\partial X^i$ by suitable differentiation of Eq. (7), and setting the coefficients of $\partial^k \theta_m/\partial X^k$ to zero for each k, the following set of defining differential equations for the functions $f_k(\tau, Y)$ may be obtained:

$$\frac{\partial f_k}{\partial \tau} + \mathrm{P} \frac{\partial f_k}{\partial Y} = \frac{\partial^2 f_k}{\partial Y^2} - U f_{k-1} + \frac{1}{\mathrm{Pe}^2} f_{k-2} - \sum_{i=1}^{k} K_i(\tau) f_{k-i} \qquad (k = 0, 1, 2, \ldots) \tag{9}$$

The initial and boundary conditions on the functions $f_k(\tau, Y)$ and $\theta_m(\tau, X)$ may be determined from Eqs. (4) to (6). Using Eqs. (6) and (4a),

$$\theta_m(0, X) = \frac{1}{2} \int_{-1}^{+1} \theta(0, X, Y)\, dY$$

$$= \frac{H_1(X)}{2} \int_{-1}^{+1} H_2(Y)\, dY \tag{10}$$

Upon setting

$$f_k(0, Y) = 0 \qquad (k = 1, 2, 3, \ldots) \tag{11}$$

Eq. (5) leads to

$$f_0(0, Y) = \frac{\theta(0\, X, Y)}{\theta_m(0, X)} = \frac{2H_2(Y)}{\int_{-1}^{+1} H_2(Y)\, dY} \tag{12}$$

Furthermore, from Eqs. (4b), (4c), and (5),

$$\frac{\partial f_k}{\partial Y}(\tau, 1) = \mathrm{P} f_k(\tau, 1) \tag{13a}$$

$$\frac{\partial f_k}{\partial Y}(\tau, -1) = \mathrm{P} f_k(\tau, -1) \tag{13b}$$

and the definition of θ_m requires

$$\int_{-1}^{+1} f_k(\tau, Y)\, dY = 2\delta_{k0} \qquad (k = 0, 1, 2, \ldots) \tag{14}$$

Also, from Eq. (4d)

$$\frac{\partial^k \theta_m}{\partial X^k}(\tau, \infty) = 0 \qquad (k = 0, 1, 2, \ldots) \tag{15}$$

By solving the defining differential Eq. (9) along with the appropriate initial and boundary conditions given by Eqs. (11) to (14), the f_k's may be determined in principle by straightforward methods and hence the required coefficients $K_i(\tau)$ in Eq. (7) can be calculated using Eq. (8). Equation (7) then can be solved for $\theta_m(\tau, X)$, and $\theta(\tau, X, Y)$ may be calculated from Eq. (5).

The Function f_0

Since the defining equations for $f_0(\tau, y)$ are independent of the velocity field, we may solve for this function immediately. The detailed solution obtained in Ref. *23* is reported in the Appendix. The Appendix also lists the asymptotic steady-state representation of this function, $f_0(\infty, y)$, in Eq. (A–16).

Steady Flow

In principle, one may solve the system of equations for $f_k(\tau, Y)$ for any velocity field $U(\tau, Y)$. However, the details would be quite complex. In this work the methods are illustrated for a simple but practically useful case, namely, steady laminar flow. In this case the velocity distribution is given by

$$u(t, y) = u(y) = u_0\left(1 - \frac{y^2}{b^2}\right) \tag{16}$$

so that

$$U(\tau, Y) = U(Y) = 1 - Y^2 \tag{17}$$

Here, the reference velocity u_0 has been chosen as the centerline velocity. Using this velocity distribution, $K_1(\tau)$, $f_1(\tau, Y)$, and $K_2(\tau)$ have been calculated. The details are reported in the Appendix. After calculating these functions, one may, in principle, calculate $f_2(\tau, Y)$, $K_3(\tau)$, and so on, but the details become intractable. Fortunately, it has been shown in earlier applications of generalized dispersion theory (*20*, *21*, *24*) that Eq. (7) can be truncated after the term involving $K_2(\tau)$ on the right-hand side. Such a truncation results in

$$\frac{\partial \theta_m}{\partial \tau} = K_1(\tau)\frac{\partial \theta_m}{\partial X} + K_2(\tau)\frac{\partial^2 \theta_m}{\partial X^2} \tag{18}$$

The validity of this truncation for this problem will be examined later.

Equation (18) can be solved along with Eqs. (10) and (15) after using the following transformations:

$$X_1(X, \tau) = X + \eta(\tau) \tag{19a}$$

where

$$\eta(\tau) = \int_0^\tau K_1(\gamma)\, d\gamma \tag{19b}$$

and

$$\xi(\tau) = \int_0^\tau K_2(\gamma)\, d\gamma \tag{20}$$

The result is

$$\theta_m(\tau, X; \mathrm{P}, \mathrm{Pe}) = \frac{1}{4\sqrt{\pi\xi}}\left[\int_{-1}^{+1} H_2(Y)\,dY\right]\int_0^{\infty} H_1(X_1') \cdot \exp\left[\frac{-(X_1' - X_1)^2}{4\xi}\right] dX_1' \tag{21}$$

The Peclet number (Pe) enters the model only as an additive contribution of the form $1/\mathrm{Pe}^2$ to the dispersion coefficient $K_2(\tau)$ in Eq. (A–30).

Uniform Initial Distribution

The initial distribution has already been assumed to be uniform in the z-coordinate. For the purposes of illustration, a specific initial distribution in the x- and y-coordinates has to be chosen. It will be assumed that a colloid of mass M is introduced at $x = 0$ uniformly in the y-and z-coordinates. This type of an initial distribution will simulate the experiments of Caldwell et al. (*6*) and Kesner et al. (*7*) to a good approximation.

If the reference concentration c_0 is chosen as

$$c_0 = \frac{M}{2b^2 a\mathrm{Pe}} \tag{22}$$

the initial distribution functions h_1 and h_2 may be written as

$$h_1(x) = \frac{b^2 u_0}{D}\,\delta(x) \tag{23a}$$

$$h_2(y) = 1 \tag{23b}$$

The dimensionless counterparts, therefore, are

$$H_1(X) = \delta(X) \tag{24a}$$

$$H_2(Y) = 1 \tag{24b}$$

Fof $H_2(Y)$ given by Eq. (24b), Eq. (A–14) for A_n in the Appendix simplifies to

$$\left.\begin{aligned} A_n &= \frac{1}{\lambda_n^4}\left(\mathrm{P}^2\alpha_n \cosh\frac{\mathrm{P}}{2}\sin\alpha_n\right) \qquad (\text{odd } n) \\ &= \frac{1}{\lambda_n^4}\left(2\mathrm{P}\alpha_n^2 \sinh\frac{\mathrm{P}}{2}\cos\alpha_n\right) \qquad (\text{even } n) \end{aligned}\right\} \tag{25}$$

When Eqs. (24) are introduced in Eq. (21), the solution for θ_m may be written as

$$\theta_m = \frac{1}{2\sqrt{\pi\xi}} \exp\left[\frac{-X_1^2}{4\xi}\right] \tag{26}$$

Some Asymptotes

For large values of τ, Eq. (A–18) from the Appendix reads

$$\underset{\tau \to \infty}{Lt}\ K_1(\tau; \mathrm{P}) = K_1(\infty; \mathrm{P}) = \frac{2}{\mathrm{P}^2}(1 - \mathrm{P} \coth \mathrm{P}) \tag{A–18}$$

For small P, Eq. (A–18) may be approximated by

$$K_1(\infty; \mathrm{P}) \approx -\frac{2}{3} - \frac{\mathrm{P}^2}{15} \tag{27}$$

Hsieh (*25*) analyzed dispersion in an open channel in the absence of any fields using generalized dispersion theory. By symmetry, the results of this work for a parallel plate channel for P = 0 should agree with those of Hsieh. This has been verified for all the results presented in Ref. *23*. For instance, Eq. (27) shows that as P → 0, $K_1(\infty; \mathrm{P}) \to -2/3$ which is the expected result. For large P, Eq. (A–18) may be approximated by

$$K_1(\infty; \mathrm{P}) \approx \frac{2}{\mathrm{P}^2}(1 - \mathrm{P}) \tag{28}$$

Similarly, the following results may be derived for $K_2(\infty; \mathrm{P}, \mathrm{Pe})$ from Eq. (A–31) in the Appendix. For small P,

$$K_2(\infty; \mathrm{P}, \mathrm{Pe}) \approx \frac{1}{\mathrm{Pe}^2} + \frac{8}{945} + \frac{4\mathrm{P}}{135} \tag{29}$$

and for large P,

$$K_2(\infty; \mathrm{P}, \mathrm{Pe}) \approx \frac{1}{\mathrm{Pe}^2} + \frac{8}{\mathrm{P}^6}(\mathrm{P}^2 - 5\mathrm{P} + 7) \tag{30}$$

Comparison with the Theory of Giddings et al.

It is of interest to compare the results of this work with those of Giddings et al. (*16*) which have been derived using the nonequilibrium theory proposed by Giddings (*14*). This theory is asymptotically valid in the limit of large τ.

TABLE 1

Correspondence between the Symbols of Giddings et al. (*16*) and Those of This Work

Giddings et al. (*16*)	This work
λ	$\frac{1}{2\mathrm{P}}$
$\mu(\zeta) - 1$	$\frac{\{1 - Y^2 + K_1(\infty)\}}{-K_1(\infty)}$
c^*/c_0^*	$\left(\frac{e^{-\mathrm{P}} \sinh \mathrm{P}}{\mathrm{P}}\right) f_0(\infty, Y)$
R	$-3K_1(\infty)/2$
ϕ	$\frac{-\mathrm{P}^2 f_1(\infty, Y)}{K_1 f_0(\infty, Y)}$
χ	$-\frac{3}{4}\frac{K_2(\infty)}{K_1(\infty)}$
ψ	$\frac{2K_2(\infty)\mathrm{P}^2}{K_1^2(\infty)}$
H	$\frac{2bK_2(\infty)\mathrm{Pe}}{-K_1(\infty)}$

From basic definitions, the correspondence reported in Table 1 has been established between the symbols used by Giddings et al. and those of this work. It has been verified by actual comparison that the expressions derived by Giddings et al. (*16*) for the quantities in Table 1 in terms of system variables and parameters are accurate. It should be emphasized that the present work is more general in scope than the asymptotic non-equilibrium theory, and is capable of predicting system behavior, in principle, from time zero without recourse to intuitive assumptions.

RESULTS AND DISCUSSION

It is seen from the analysis that the dimensionless colloid concentration in the channel is a function of dimensionless time τ and the dimensionless axial coordinate X; it will also depend on the two characteristic parameters—transverse Peclet number P, and axial Peclet number Pe. The dependence on Pe occurs only through an additive contribution of $1/\mathrm{Pe}^2$ to the axial dispersion coefficient whereas the dependence on P is quite complex. It is seen from Eq. (18) that the average concentration of the colloid is convected downstream in the channel with a time-dependent dimensionless velocity $-K_1(\tau)$ and spreads axially with respect to its center of gravity with a time-dependent dimensionless dispersion coefficient $K_2(\tau)$. The behavior of these coefficients should, therefore, yield

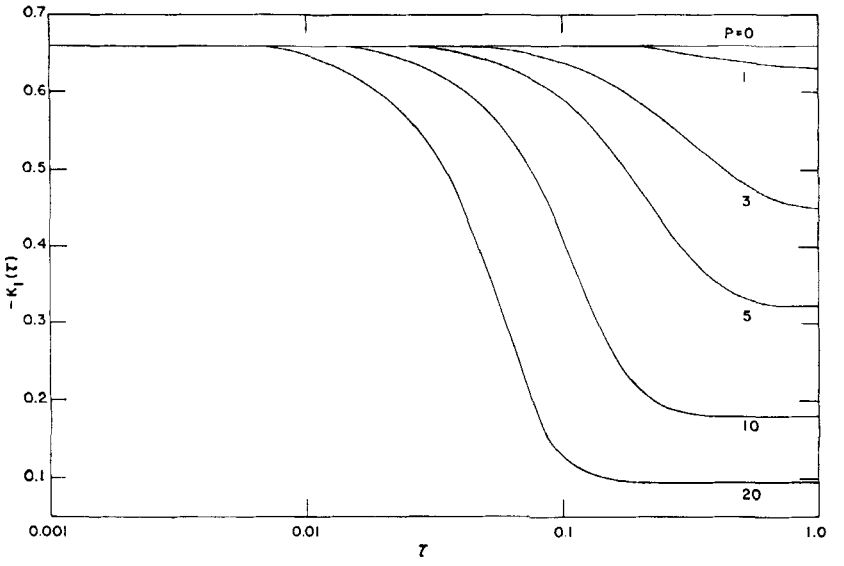

FIG. 2. Plot of the dimensionless convective coefficient $K_1(\tau)$ as a function of dimensionless time τ, from Eq. (A-17) for P = 0, 1, 3, 5, 10, and 20.

physical insight into the transport of colloid in the FFF column. With this aim in view, Eqs. (A–17), (A–18), (A–30), and (A–31) have been used to obtain the data plotted in Figures 2, 3, 4, and 5, respectively. The data were calculated using Double Precision Arithmetic on an IBM 360/65 (*23*).

Figure 2 shows the transient approach of K_1 to its steady-state value for various representative values of the transverse Peclet number P. The range of P values runs from 0 to 20. (It may be mentioned that for the experiments of Kesner et al. in EFFF systems, the P values range from 0 to 12 or so.) At time zero, the initial distribution is uniform so that the average velocity of the colloid is equal to the average flow velocity; therefore, $-K_1$, which is the ratio of the average velocity of the colloid to the centerline velocity in the flow, is $\frac{2}{3}$. For P = 0, the axial velocity of the colloid remains at the same value for all time. For P $\neq$ 0, as time increases, the colloid migrates toward the boundary $Y = 1$ and its concentration distribution is weighted more and more toward the slower moving region near the upper boundary. Therefore, the average velocity of the colloid decreases monotonically with increasing time toward its asymptotic steady-state value. As expected, the larger the value of P, the smaller the

axial velocity of the colloid. The figure clearly shows that the relaxation time required for K_1 to reach its asymptotic steady-state representation *decreases with increasing P*. In general, from physical reasons, this relaxation time can be seen to be the larger of the following two characteristic times.

(a) The time required for the colloid to migrate from one membrane to the other due to the field.

(b) The time required for equilibration due to Brownian motion across the asymptotic distribution of the colloid in the Y coordinate.

In dimensionless terms, the τ required for (a) is given by

$$\tau_s \simeq 2/\mathrm{P} \tag{31}$$

while the τ for (b) may be estimated roughly as

$$\tau_s \simeq 1/\mathrm{P}^2 \tag{32}$$

if the characteristic width of the asymptotic distribution is taken to be b/P as assumed by other workers. Equation (32) represents case (b) only when $\mathrm{P} \gg 1/2$. When P is on the order of 1 or smaller, the colloid is practically distributed over the entire cross section of the channel, and hence the relaxation time for equilibration by Brownian motion would be given by

$$\tau_s \approx 1 \tag{33}$$

Comparison of Eqs. (31) to (33) shows that the relaxation time is governed by criterion (a) when $\mathrm{P} \gg 1/2$, which is the case in most FFF systems of practical interest. Figure 1 shows that the relaxation time for K_1 for $\mathrm{P} \gtrsim 1$ is, in fact, on the order of magnitude of the result given in Eq. (31).

Figure 3 shows the asymptotic $K_1(\infty)$ plotted against P along with the approximations developed in Eqs. (27) and (28) for this quantity in the limits of small and large P. The approximations can be seen to be quite good over a wide range of the parameter P. It should be noted here that $K_1(\infty)$ is linearly related to the retention parameter R used by Giddings as shown by Table 1.

The dimensionless axial dispersion coefficient $K_2(\tau)$ is a function of the transverse Peclet number P and the axial Peclet number Pe in addition to depending on τ. However, the dependence on Pe occurs due to the additive contribution of axial molecular diffusion to axial dispersion. This dependence can be isolated by simply subtracting $1/\mathrm{Pe}^2$ from K_2 so

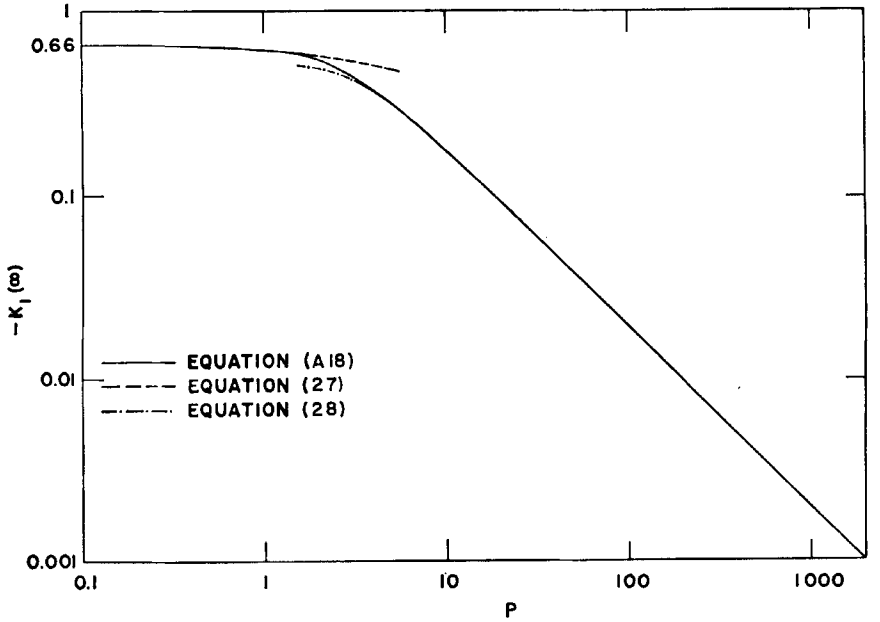

FIG. 3. Plot of the dimensionless steady-state convective coefficient $K_1(\infty)$ as a function of P from the exact result (Eq. A-18), the small P approximation (Eq. 27), and the large P approximation (Eq. 28).

that the result is only a function of τ and P. Figure 4 shows the behavior of $K_2 - (1/Pe^2)$ as a function of τ for various values of P. The results for $P = 0$ correspond to those of Hsieh (*25*) in the absence of a field. In all cases when $P \neq 0$ (in the presence of a field), the figure shows that for very small times the axial dispersion coefficient is practically identical to that for the case $P = 0$ (no field). As time increases, axial dispersion appears to be enhanced slightly in comparison to the case of no field and then decreases substantially for large time, resulting in lower asymptotic dispersion coefficients in the presence of a field. This behavior may be explained as follows. For very small τ, the field has not had much of an effect; therefore, the axial dispersion coefficient is nearly the same as that in the absence of the field. As time increases, at intermediate times the colloid migrates in the presence of the field so that it is distributed more favorably in the large velocity gradient region near the upper boundary but is still present in sufficient quantities all over the cross section. This explains the increased dispersion compared to the case $P = 0$ because

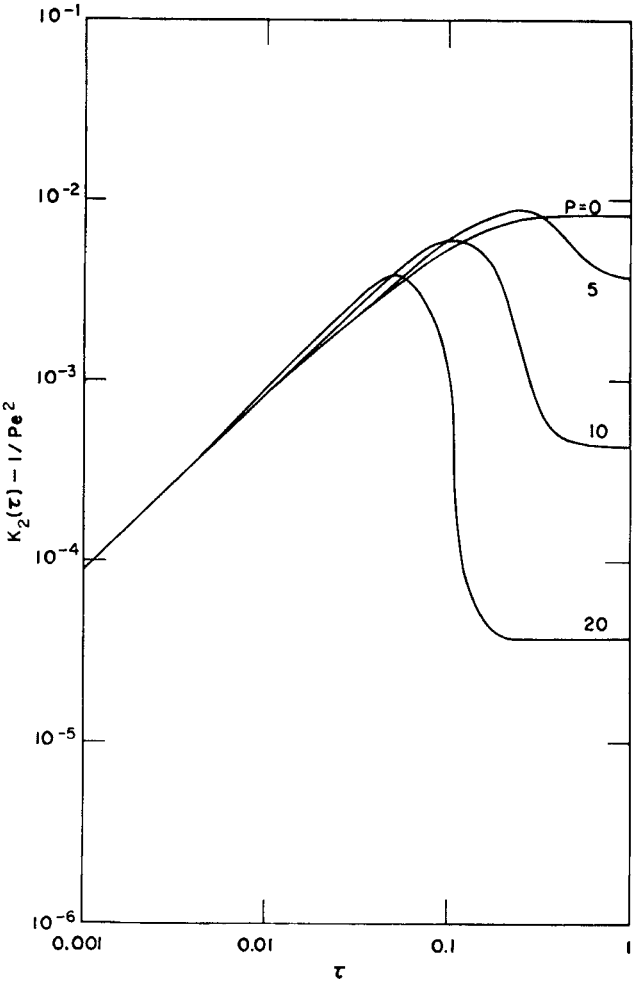

FIG. 4. Plot of the dimensionless dispersion coefficient $K_2(\tau) - (1/Pe^2)$ as a function of dimensionless time τ from Eq. (A-30) for P = 0, 5, 10, and 20.

larger velocity gradients enhance dispersion. However, as time increases, the colloid tends to form a distribution *heavily weighted* in the slower-moving region near the upper boundary. The reduced transverse extent of the colloid, along with the fact that the velocities are low in this region, contributing to very small net velocity variations across the colloid distribution, results in a substantial reduction of axial dispersion. The figure shows that the asymptotic value of the dispersion coefficient for P = 0 is more than a hundred times the value for P = 20, thus indicating a *dramatic reduction in axial dispersion for highly retained colloids.* Figure 4 also shows that K_2 relaxes to its asymptotic steady state at earlier values of τ for larger P. The relaxation times are about the same as those for K_1 for the same values of P and may be predicted by Eq. (31) except when P is very small. For convenience, the dependence of the large-time asymptote of K_2 $-(1/\mathrm{Pe}^2)$ on P is shown in Fig. 5. Also shown in this figure are the small and large P approximations developed in Eqs. (29) and (30).

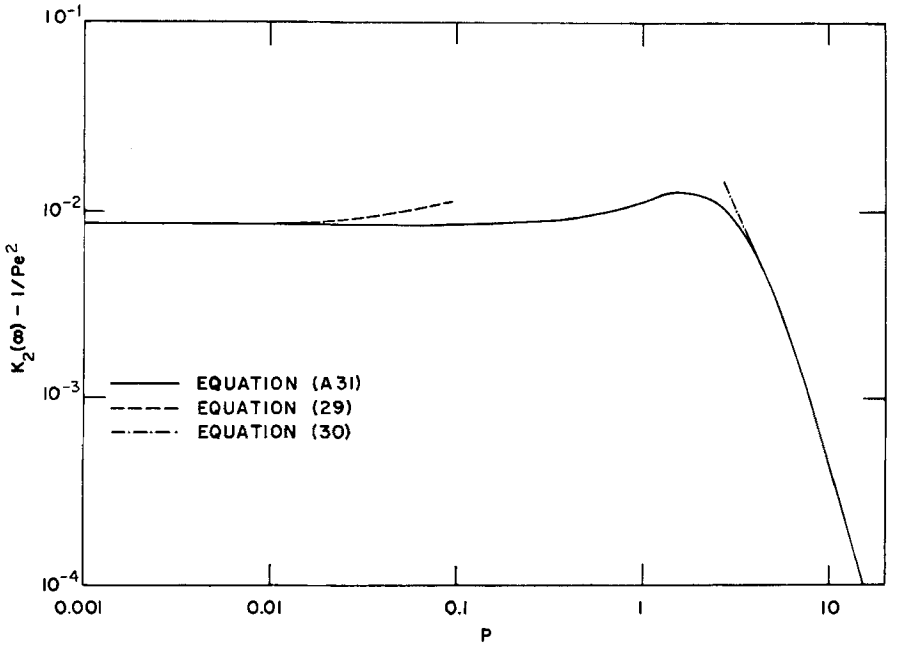

FIG. 5. Plot of the steady-state dispersion coefficient $K_2(\infty) - (1/\mathrm{Pe}^2)$ as a function of P from the exact result (Eq. A-31), the small P approximation (Eq. 29), and the large P approximation (Eq. 30).

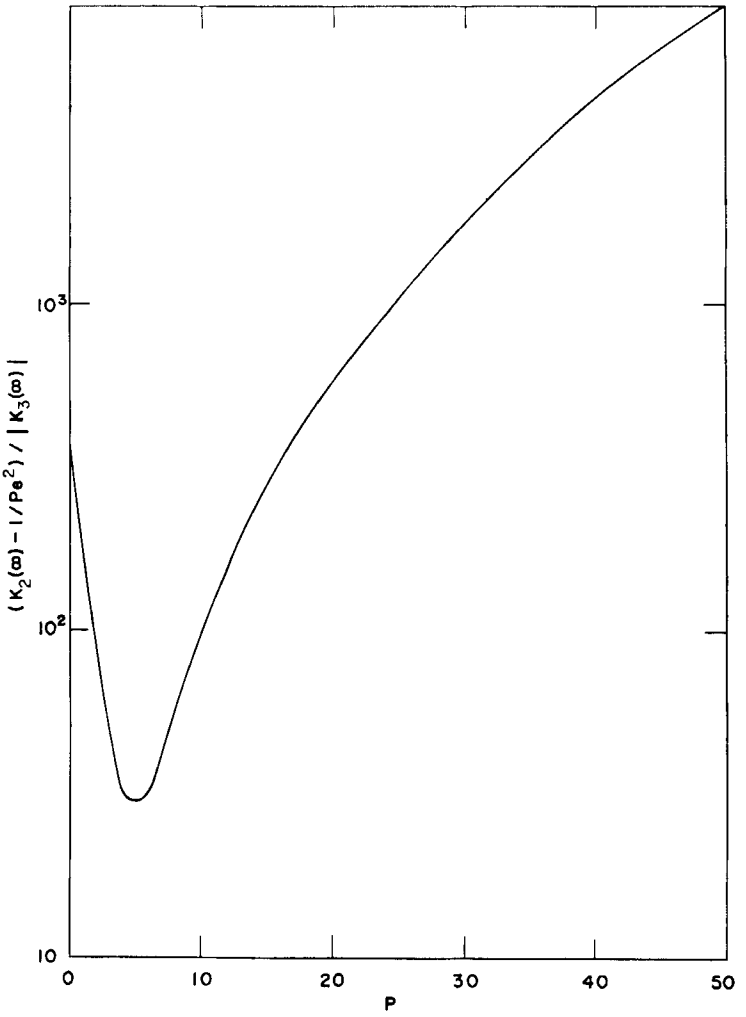

FIG. 6. Plot of the ratio of the steady-state coefficients $[K_2(\infty) - (1/\mathrm{Pe}^2)]/|K_3(\infty)|$ as a function of P.

It was mentioned earlier that the validity of truncating Eq. (7) for $i > 2$ would be examined for this work. One way of establishing this is to demonstrate that $K_3(\tau) \ll K_2(\tau)$. The evaluation of the coefficient $K_3(\tau)$ involves the use of the function $f_2(\tau, Y)$, which is extremely difficult to obtain. However, Eqs. (8) and (11) show that K_3 and all the higher coefficients are zero at time zero while $K_2 = 1/\mathrm{Pe}^2$. Therefore, for small times it probably is reasonable to perform the truncation involved. In view of the complexity of the task, only $K_3(\infty)$ was examined in this work. A numerical scheme was used to calculate $f_2(\infty, Y)$, and $K_3(\infty)$ was obtained by using Simpson's rule for the integration required in Eq. (8). Figure 6 shows a plot of the ratio $[K_2(\infty) - (1/\mathrm{Pe}^2)]/|K_3(\infty)|$ as a function of P. The figure shows this ratio to reach a minimum of 50 around $\mathrm{P} \simeq 5$. This ratio still is comfortably large to justify the truncation. However, this supportive evidence for the truncation should be interpreted with caution since the derivative $\partial^3\theta_m/\partial X^3$ can be much larger than $\partial^2\theta_m/\partial X^2$ at very small values of τ. The best test of the truncated model for θ_m will, of course, be comparison with suitable experimental data.

Comparison with Asymptotic Theory

As pointed out before, earlier mathematical modeling efforts in FFF have been confined to the analysis of asymptotic large τ behavior. That is, in effect, the average concentration distribution is assumed to satisfy the model

$$\frac{\partial\theta_m}{\partial\tau} - K_1(\infty)\frac{\partial\theta_m}{\partial X} = K_2(\infty)\frac{\partial^2\theta_m}{\partial X^2} \tag{34}$$

The solution of this equation (with the same initial and boundary conditions imposed on the exact model for θ_m) may be written as

$$\theta_m(\tau, X) = \frac{1}{2\sqrt{K_2(\infty)\tau}}\exp\left[\frac{(X + K_1(\infty)\tau)^2}{4K_2(\infty)\tau}\right] \tag{35}$$

Comparison with the exact solution from Eq. (26) shows that the approximations being made are

$$\eta(\tau) \simeq K_1(\infty)\tau \tag{36}$$

$$\xi(\tau) \simeq K_2(\infty)\tau \tag{37}$$

The percentage error made in using Eq. (36), that is, $\{[K_1(\infty)\tau - \eta(\tau)]/\eta(\tau)\} \times 100$, is plotted as a function of τ in Fig. 7 for various values of P.

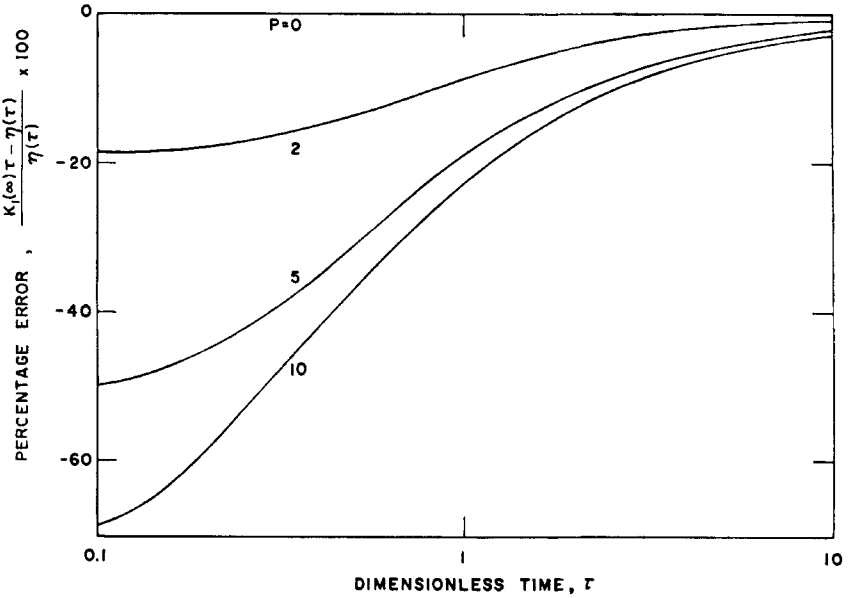

FIG. 7. Plot of the percentage error in approximating $\int_0^\tau K_1(\tau)\,d\tau$ by $K_1(\infty)\tau$ as a function of dimensionless time τ for P = 0, 2, 5, and 10.

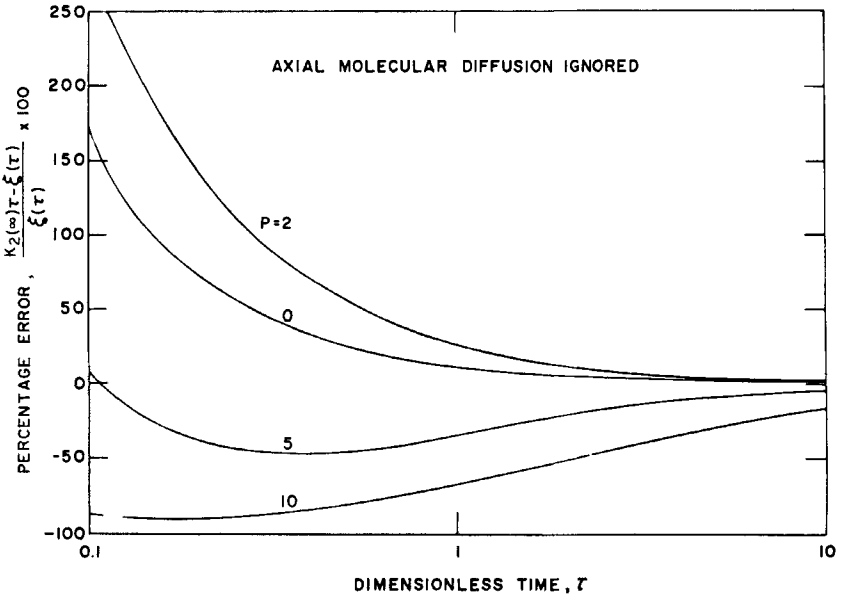

FIG. 8. Plot of the percentage error in approximating $\int_0^\tau K_2(\tau)\,d\tau$ by $K_2(\infty)\tau$ as a function of dimensionless time τ for P = 0, 2, 5, and 10; Pe = ∞.

The figure reveals that this approximation gets progressively worse as P increases *in spite of the fact that relaxation times are smaller for larger P.* This is clearly because of the smaller asymptotic values reached by K_1 for larger P.

Figure 8 shows plots of $[K_2(\infty)\tau - \xi(\tau)]/\xi(\tau) \times 100$ as a function of P when axial molecular diffusion is ignored. Since the axial dispersion coefficient, in this case, starts from a value of 0 at time 0, increases for a while, and then decreases to the asymptotic value, the behavior of this error is more complex. It is important to note that, in general, the errors are much larger in approximating $K_2(\tau)$ with the asymptotic value than in the case of K_1.

Figure 9 shows breakthrough (or elution) curves at $X = 1$ for Pe = 1000 for two different values of P (5 and 15) calculated from the exact solution with the time variable K_1 and K_2 and the asymptotic model which uses $K_1(\infty)$ and $K_2(\infty)$. It is clear from the figure that even at values of τ on the order of 10, which are far beyond the relaxation times involved, the

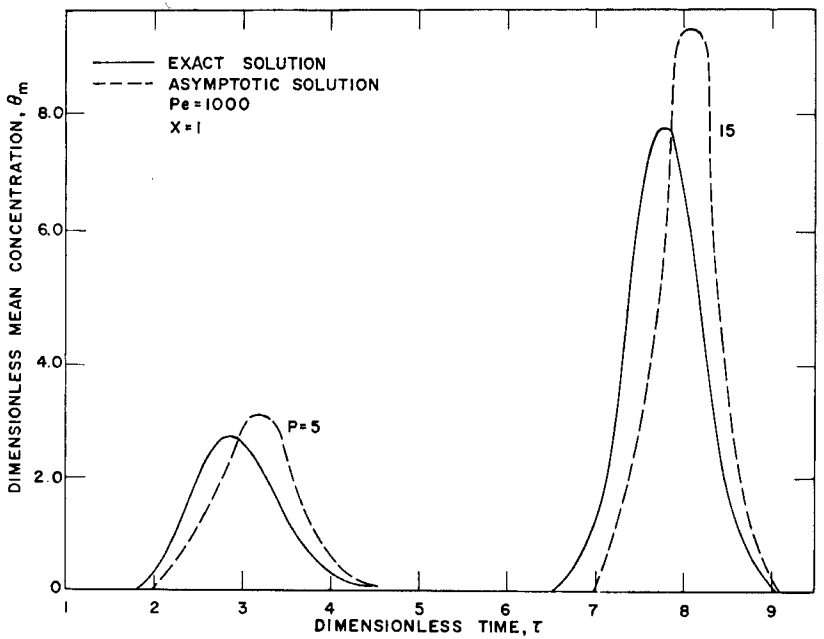

FIG. 9. Breakthrough curves from the exact solution (Eq. 26) and the asymptotic solution (Eq. 35) for P = 5 and 15.

asymptotic model is quite inadequate in describing the concentration distribution. Krishnamurthy (*23*) shows that one needs to go to much farther axial stations ($X = 5$) in order to adequately represent the concentration distributions using the asymptotic result from Eq. (35) for such P values.

Height Equivalent of a Theoretical Plate

A popular concept in chromatography is the "height equivalent of a theoretical plate," H. Giddings (*17*) has shown how this concept, while it has no association with reality, can still be useful as a measure of axial spreading in chromatographic columns. Using his definition and the asymptotic results from his theory, he has obtained expressions for this quantity in FFF systems. H may be defined in terms of the variance of the solute distribution and the length of the column as

$$H = \sigma^2/L \tag{38}$$

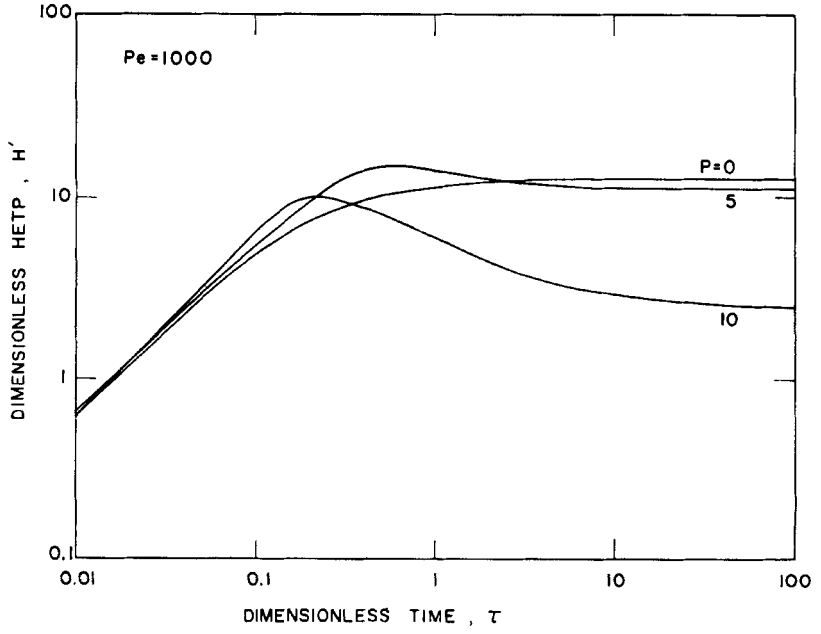

FIG. 10. Plot of the dimensionless height equivalent of a theoretical plate H' as a function of dimensionless time τ for P = 0, 5, and 10.

From Eqs. (19b), (20), and (26), a dimensionless form of H can be shown to be given by

$$H' = H/2b = \xi \mathrm{Pe}/(-\eta) \tag{39}$$

It should be noted that this quantity is a function of time, and it undergoes relaxation to its asymptotic value for large τ. The behavior of H' as a function of time τ is illustrated in Fig. 10 for representative values of the parameter P. It is clear from the figure that using asymptotic results for H' can lead to large errors in predicting system performance under certain conditions.

Comparison of Theory with Experiments

A substantial amount of experimental data is available on FFF systems in the literature in the form of retention volumes or R values, plate heights, and elution curves from FFF columns (*2–10*). Typically, these columns are long enough so that the time period between introduction and elution of the colloid is on the order of magnitude of the relaxation time for the system, or larger. Under these conditions, Giddings and co-workers show, in the above references, that the asymptotic nonequilibrium theory predicts retention data quite well (in electrical FFF columns where deviations have been observed, they have offered possible explanations). The theory usually underpredicts axial dispersion data reported in the form of plate heights, and explanations have been presented to account for the observed disagreement between theory and experiment. It is clear that for large enough values of time, the predictions of the present theory would completely agree with those of the nonequilibrium theory. Therefore, a precise test of the present theory has to await the availability of calibrated elution curves in systems where the time interval between injection and elution is suitably small. In this work a comparison of the predictions of our theory will be made with the experimental elution curves from Caldwell et al. (*6*) and Kesner et al. (*7*) obtained from parallel membrane electrical FFF systems. For the reasons described below, these comparisons can only be semiquantitative in nature. The data available are in the form of UV-recorder responses as a function of time at the system exit. Calibration information is not available, but the response of the recorder may be assumed to be linear in protein concentration in the range of concentrations involved so that a comparison can be made by matching the peak heights in the breakthrough curves on an individual basis for each protein. Also, Figs. 7 and 8 in Kesner et al. (*7*) show that

under identical operating conditions, proteins such as albumin and hemoglobin arrive at quite different times at the system exit depending on whether γ-globulin is present or not. This suggests colloidal interactions or variations in operating parameters that were undetectable. Hence the comparisons to be made here can only be indicative of trends and cannot be interpreted precisely. Furthermore, Kesner et al. observed that the peak arrival times from their experimental data matched theoretical predictions made from nonequilibrium theory (with the aid of literature data on the physical and electrical properties of the proteins) only for their runs at a pH = 8.0. For experiments at a pH = 4.5, they observed substantial deviations for which they offer some possible explanations. In any case, we *estimated P values for comparison at a pH of 8.0 from literature data for electrophoretic mobilities and diffusivities for the various proteins compiled in Kesner's thesis* (*26*). The resulting comparison is shown in Fig. 11 for the separation of γ-globulin and albumin. Figures 12 and 13 show comparisons of theory with experiment for some more protein separations, this time at a pH of 4.5. The theoretical results for these comparisons were calculated using a P estimated from the experimental data points in the l/w vs $1/E$ plots of Kesner et al. In all three figures the slight deviations in matching the peak arrival times may be attributed to:

(a) The fact that the predictions are based on the exact theory whereas the P values were estimated from the l/w vs $1/E$ data in which the ordinate had been calculated using the asymptotic nonequilibrium theory.

(b) The possible errors we made in reading the data for P off the graphs of Kesner et al.

Considering the restrictions mentioned earlier, the theory makes reasonable predictions of the axial dispersion observed in the experiments, especially at small P. At larger P values the experimental dispersion is much larger than that predicted by theory. It is possible that this trend of larger deviations at larger P could be the result of the various simplifying assumptions made in developing the theory. However, one possible explanation could be that the observed experimental dispersion is caused by additional Taylor dispersion in the connecting tubing from the injection station to the channel inlet, and in the tubing from the channel exit to the UV-recorder. Since, for large P, axial dispersion in the FFF column itself is substantially reduced (by a factor of approximately 20 for P = 10 when compared with P = 0), Taylor dispersion in the connecting tubing, where there is no applied field, would take on an increased importance.

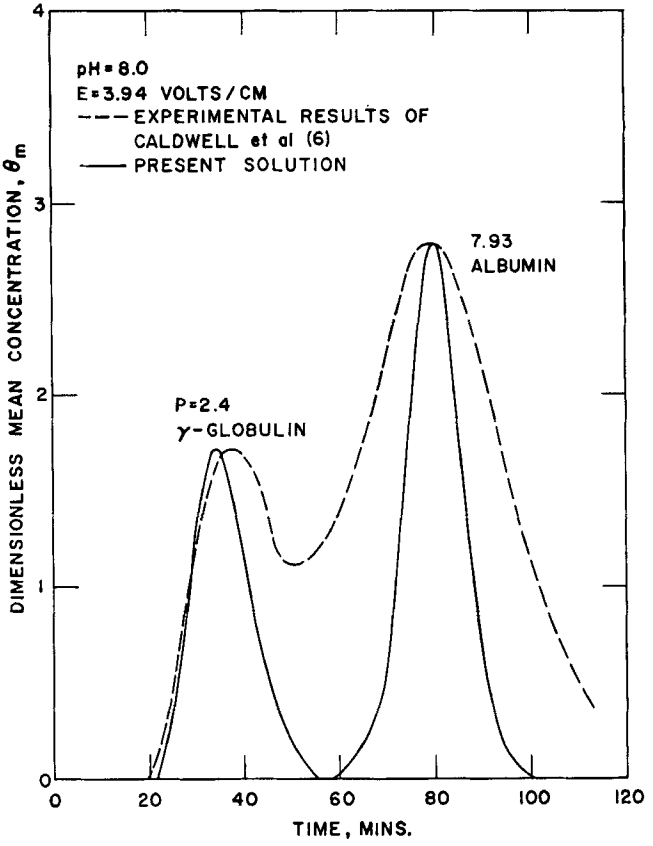

FIG. 11. Breakthrough curves from present solution (Eq. 26) and experimental results of Caldwell et al. (6) for γ-globulin and albumin.

In other words, a short length of such tubing which causes very little additional dispersion in chromatographic systems could possibly play an overriding role in determining the extent of peak spreading in an FFF column. Of course, even with accurate data on the length and diameter of this tubing, it would be very difficult to make a proper estimate of its contribution because of the changes in geometry. One way of testing the conjecture made here is to compare peak spreading in the case of a run with a high value of P [such as the one for γ-globulin in Fig. 8 of Kesner et al. (7)] using different sizes of connecting tubing.

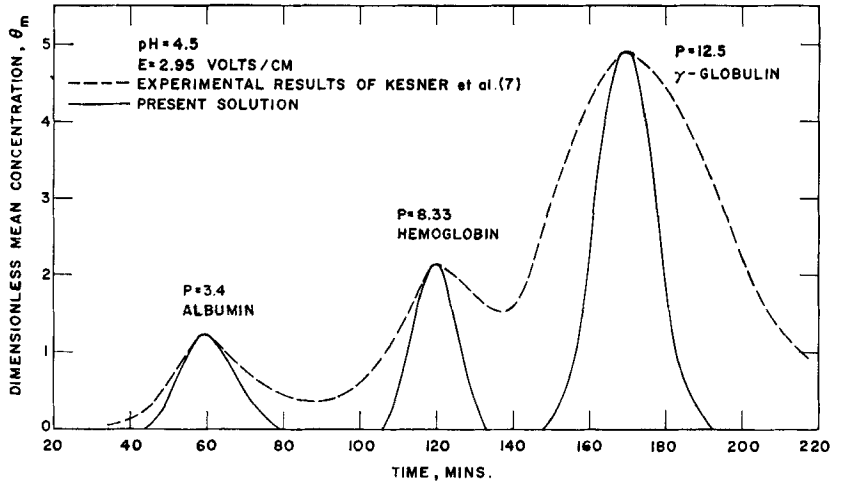

FIG. 12. Breakthrough curves from the present solution (Eq. 26) and the experimental results of Kesner et al. (7) for albumin, hemoglobin, and γ-globulin.

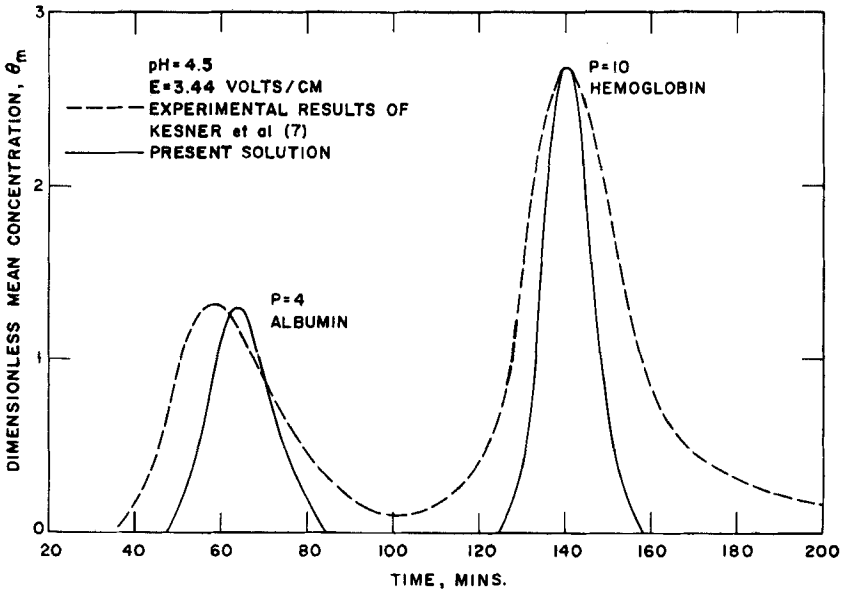

FIG. 13. Breakthrough curves from the present solution (Eq. 26) and the experimental results of Kesner et al. (7) for albumin and hemoglobin.

Other explanations for the large observed dispersion could be side wall effects, or successive disturbances which would cause the colloidal distributions to undergo relaxations—as noted in this work, the axial dispersion coefficient is usually much larger during the relaxation stage than in the asymptotic stage.

Finally, it should be reemphasized that the above comparisons are not to be interpreted as precise tests of the theory. Such testing must await the availability of more quantitative experimental data on FFF systems in the region of time where the coefficients K_1 and K_2 exhibit transient behavior.

CONCLUSIONS

The unsteady transport of a colloid introduced into a fluid in time-dependent flow in a parallel plate channel in the presence of a transverse field has been analyzed using generalized dispersion theory. The present treatment provides a rigorous unified theoretical foundation for the modeling of field-flow fractionation (FFF) devices.

The results from the theory show that the dimensionless average concentration of the colloid depends on dimensionless time and axial position; it also depends parametrically on the transverse Peclet number P and the axial Peclet number Pe.

For large values of time, the results of the present work have been shown to approach those of the nonequilibrium theory of Giddings asymptotically. In the case of steady laminar flow and a uniform initial distribution, numerical results show that the errors involved in using the asymptotic theory increase substantially with increasing P. An attempt has been made to compare the theoretical predictions with the data of Giddings and co-workers on electrical FFF columns. The comparisons show the theory to be reasonably successful in predicting observed axial dispersion for small P. In view of the extremely small dispersion predicted by the theory for FFF at large P, it is conjectured that one possible reason for the observed large dispersion in the experiments could be the effect of connecting tubing used between the injection port and the channel inlet and between the channel exit and the UV-monitoring device.

The methodology of generalized dispersion theory which has been used in this work is quite general, and can be used equally well to predict the performance of systems with other geometries such as the hollow fiber device of Reis and Lightfoot (*12*).

APPENDIX

The details of the various solutions for the functions f_0 and f_1 and the results for the coefficients K_1 and K_2 are presented here.

The Function $f_0(\tau, Y)$

By setting $k = 0$ in Eqs. (9), (13), and (14), and using Eq. (12), the following defining equations may be obtained for $f_0(\tau, Y)$:

$$\frac{\partial f_0}{\partial \tau} + \mathrm{P}\frac{\partial f_0}{\partial Y} = \frac{\partial^2 f_0}{\partial Y^2} \tag{A-1}$$

$$f_0(0, Y) = \frac{2H_2(Y)}{\int_{-1}^{+1} H_2(Y)\, dY} \tag{A-2}$$

$$\frac{\partial f_0}{\partial Y}(\tau, 1) = \mathrm{P} f_0(\tau, 1) \tag{A-3}$$

$$\frac{\partial f_0}{\partial Y}(\tau, -1) = \mathrm{P} f_0(\tau, -1) \tag{A-4}$$

$$\int_{-1}^{+1} f_0(\tau, Y)\, dY = 2 \tag{A-5}$$

It may be observed that the function $f_0(\tau, Y)$ is independent of the velocity field and, therefore, Eqs. (A-1) to (A-5) may be solved *immediately* by the method of separation of variables. The result is

$$f_0(\tau, Y) = \sum_{n=0}^{\infty} A_n \exp(-\lambda_n^2 \tau)\, \phi_n(Y) \tag{A-6}$$

where

$$\lambda_n^2 = \alpha_n^2 + \frac{\mathrm{P}^2}{4} \tag{A-7}$$

$$\alpha_0^2 = -\frac{\mathrm{P}^2}{4} \tag{A-8}$$

$$\alpha_n^2 = \frac{n^2\pi^2}{4} \qquad (n = 1, 2, 3, \ldots) \tag{A-9}$$

and the eigenfunctions $\phi_n(Y)$ are given by

$$\phi_n(Y) = e^{\mathrm{P}Y/2}(\cos \alpha_n Y + G_n \sin \alpha_n Y) \tag{A-10}$$

Here

$$\left.\begin{aligned} G_n &= \frac{2\alpha_n}{-\mathrm{P}} \qquad (\text{odd } n) \\ &= \frac{\mathrm{P}}{2\alpha_n} \qquad (\text{even } n) \end{aligned}\right\} \tag{A-11}$$

It should be noted that, when $n = 0$, Eq. (A–10) may be conveniently rewritten as

$$\phi_0(Y) = e^{\mathrm{P}Y} \tag{A-12}$$

The expansion coefficients A_n are obtained using the orthogonality property of the set of eigenfunctions ϕ_n. This set appears to be complete even though the Sturm-Liouville system for ϕ_n is not proper in view of Eq. (A–3).

$$A_n = \frac{\int_{-1}^{+1} r(Y) f_0(0, Y) \phi_n(Y)\, dY}{\int_{-1}^{+1} r(Y) \phi_n^2(Y)\, dY} \qquad (n = 0, 1, 2, \ldots) \tag{A-13}$$

where the weighting factor is $r(Y) = e^{-\mathrm{P}Y}$. From Eqs. (A–2) and (A–12),

$$A_n = \frac{2}{\int_{-1}^{+1} H_2(Y)\, dY} \frac{\int_{-1}^{+1} H_2(Y) e^{-\mathrm{P}Y} \phi_n(Y)\, dY}{\int_{-1}^{+1} e^{-\mathrm{P}Y} \phi_n^2(Y)\, dY} \tag{A-14}$$

It may be noted that A_0 is independent of the initial distribution and is given by

$$A_0 = \frac{\mathrm{P}}{\sinh \mathrm{P}} \tag{A-15}$$

Asymptotically as $\tau \to \infty$, $f_0(\tau, Y)$ approaches a steady-state distribution given by

$$f_0(\infty, Y) = \frac{\mathrm{P}}{\sinh \mathrm{P}} e^{\mathrm{P}Y} \tag{A-16}$$

The Coefficient $K_1(\tau)$

For steady laminar flow, the parabolic velocity profile is given by Eq. (17). Using this velocity field, $K_1(\tau)$ may be calculated immediately from Eq. (8) as

$$\begin{aligned} K_1(\tau) &= -\frac{1}{2} \int_{-1}^{+1} (1 - Y^2) f_0(\tau, Y)\, dY \\ &= K_1(\infty) - \frac{1}{2} \sum_{n=1}^{\infty} A_n \exp(-\lambda_n^2 \tau)\, C_n \end{aligned} \tag{A-17}$$

where

$$K_1(\infty) = \underset{\tau \to \infty}{Lt}\, K_1(\tau) = \frac{2}{P^2}(1 - P \coth P) \tag{A-18}$$

and

$$\left.\begin{aligned} C_n &= \frac{1}{\lambda_n^3}\left[-4\lambda_n \cosh\frac{P}{2} + \frac{4P}{\lambda_n}\sinh\frac{P}{2}\right]\cos\alpha_n \qquad \text{(even } n\text{)} \\ &= \frac{1}{\lambda_n^3}\left[-\frac{8\alpha_n}{\lambda_n}\cosh\frac{P}{2} + \frac{8\alpha_n\lambda_n}{P}\sinh\frac{P}{2}\right]\sin\alpha_n \qquad \text{(odd } n\text{)} \end{aligned}\right\} \tag{A-19}$$

The coefficient $K_1(\tau)$ represents the negative of the dimensionless velocity of the solute distribution. *It is seen from Eq. (A–17) that K_1 depends on τ even though the velocity field may be steady.*

Solution for $f_1(\tau, Y)$ and $K_2(\tau)$

Setting $k = 1$ in Eq. (9) gives

$$\frac{\partial f_1}{\partial \tau} + P\frac{\partial f_1}{\partial Y} = \frac{\partial^2 f_1}{\partial Y^2} - [U(\tau, Y) + K_1(\tau)]f_0(\tau, Y) \tag{A-20}$$

This is to be solved with the conditions

$$f_1(0, Y) = 0 \tag{A-21}$$

$$\frac{\partial f_1}{\partial Y}(\tau, 1) = P f_1(\tau, 1) \tag{A-22}$$

$$\frac{\partial f_1}{\partial Y}(\tau, -1) = P f_1(\tau, -1) \tag{A-23}$$

$$\int_{-1}^{+1} f_1(\tau, Y)\, dY = 0 \tag{A-24}$$

The solution procedure, using Duhamel's theorem, is reported elsewhere (*23*). The final result for $f_1(\tau, Y)$ is

$$f_1(\tau, Y) = f_1(\infty, Y) + \sum_{n=1}^{\infty} S_n(\tau)\phi_n(Y) \tag{A-25}$$

where

$$f_1(\infty, Y) = \frac{1}{\mathrm{P}^3 \sinh^2 \mathrm{P}}\left[\left\{\left[1 - \frac{2}{\mathrm{P}}\coth \mathrm{P}\right]\mathrm{P}^3 Y - \frac{\mathrm{P}^3 Y^3}{3} + \mathrm{P}^2 Y^2 - \left[\left(\frac{\mathrm{P}^2}{3} - \mathrm{P}\coth \mathrm{P} - 1\right)2\mathrm{P}\cosh \mathrm{P} + (\mathrm{P}^2 + 4)\sinh \mathrm{P} + \mathrm{P}Q\right]\right\}e^{\mathrm{P}Y} + Q \sinh \mathrm{P}\right] \tag{A-26}$$

$$Q = -2\mathrm{P}(1 + \coth \mathrm{P})e^{-\mathrm{P}} \tag{A-27}$$

and

$$S_n(\tau) = -\left[A_n(1 + K_1(\infty))\tau - \left(\frac{\mathrm{P}C_n}{\lambda_n^2 \sinh \mathrm{P}(1 + G_n^2)}\right)\right]\exp(-\lambda_n^2 \tau) + \frac{1}{2}A_n \sum_{\substack{m=1 \\ m \neq 1}}^{\infty} A_m \frac{\exp(-\lambda_n^2 \tau) - \exp[-(\lambda_m^2 + \lambda_n^2)\tau]}{\lambda_m^2} C_m + \frac{2}{(1 + G_n^2)} \sum_{\substack{m=1 \\ m \neq 1}}^{\infty} A_m d_{mn}\left[\frac{\exp(-\lambda_m^2 \tau) - \exp(-\lambda_n^2 \tau)}{(\lambda_n^2 - \lambda_m^2)}\right] \tag{A-28}$$

where C_n is defined by Eq. (A-19) and

$$d_{mn} = (1 - G_n^2)\frac{(-1)^n}{4\alpha_n^2} + \frac{(1 + G_n^2)}{6} \qquad m = n$$

$$\left.\begin{aligned} &= (1 - G_n G_m)\left[\frac{(-1)^{(m+n)/2}}{(m + n)^2 \frac{\pi^2}{4}}\right] \\ &\quad + (1 + G_m G_n)\left[\frac{(-1)^{(m-n)/2}}{(m - n)^2 \frac{\pi^2}{4}}\right] \\ &= (G_m G_n - 1)\left[\frac{(-1)^{(m+n-1)/2}}{(m + n)^3 \frac{\pi^3}{8}}\right] \\ &\quad - (G_n G_m + 1)\left[\frac{(-1)^{(n-m-1)/2}}{(n - m)^3 \frac{\pi^3}{8}}\right] \end{aligned}\right\} \quad m \neq n$$

m odd and n odd or m even and n even

m odd and n even or m even and n odd

(A-29)

where G_n is defined by Eqs. (A–11). From Eqs. (8), (17), and (A–25),

$$K_2(\tau) = \frac{1}{\mathrm{Pe}^2} - \frac{1}{2}\int_{-1}^{+1}(1 - Y^2)f_1(\tau, Y)\,dY$$

$$= K_2(\infty) - \frac{1}{2}\sum_{n=1}^{\infty} S_n(\tau)C_n \qquad \text{(A–30)}$$

where

$$K_2(\infty) = \underset{\tau\to\infty}{Lt}\, K_2(\tau) = \frac{1}{\mathrm{Pe}^2} + \frac{4}{\mathrm{P}^4 \sinh \mathrm{P}}\left[\frac{2\mathrm{P}^2}{3 \sinh \mathrm{P}} - \frac{10 \cosh \mathrm{P}}{\mathrm{P}} + \frac{14 \sinh \mathrm{P}}{\mathrm{P}^2} + \frac{2}{\sinh \mathrm{P}} - \frac{2\mathrm{P} \cosh \mathrm{P}}{\sinh^2 \mathrm{P}} - \frac{4 \cosh^2 \mathrm{P}}{\sinh \mathrm{P}} + 6 \sinh \mathrm{P}\right] \qquad \text{(A–31)}$$

SYMBOLS

a	channel breadth
A_n	expansion coefficients defined in Eq. (A–14)
b	channel half-width
c	local concentration
c_0	reference concentration defined in Eq. (22)
C_n	coefficients defined in Eq. (A–19)
D	diffusivity
d_{mn}	constants defined by Eq. (A–29)
f_k	coefficient functions in Eq. (9)
G_n	coefficients defined in Eq. (A–11)
K_i	dimensionless coefficients defined in Eq. (8)
M	total mass of colloid released
P	transverse Peclet number; $\mathrm{P} = bv/D$
Pe	axial Peclet number; $\mathrm{Pe} = bu_0/D$
Q	coefficient defined in Eq. (A–27)
S_n	coefficient functions defined in Eq. (A–28)
t	time
U	dimensionless flow velocity; $U = u/u_0$
u	flow velocity in the x-direction
u_0	reference velocity; also the velocity at the centerline of the channel
v	transverse velocity of a colloidal specie
X	dimensionless axial coordinate, $X = xD/b^2u_0$
X_1	defined by Eq. (19a)

x axial coordinate
Y dimensionless transverse coordinate; $Y = y/b$
y transverse coordinate; see Fig. 1
z transverse coordinate; see Fig. 1

Greek Letters

α_n eigenvalues defined in Eqs. (A–8) and (A–9)
δ Dirac delta function
δ_{ij} Kronecker delta
ξ defined by Eq. (20)
η defined by Eq. (19b)
θ dimensionless local concentration
θ_m dimensionless mean concentration
λ_n defined by Eq. (A–7)
π constant; $\pi = 3.14159\ldots$
τ dimensionless time; $\tau = Dt/b^2$
ϕ_n eigenfunctions defined in Eq. (A–10)

Acknowledgments

Acknowledgment is made to the donors of the Petroleum Research Fund, administered by the American Chemical Society, for partial support of this research through PRF Grant 8363–G5. Also, one of the authors (S.K.) was supported in part by Texaco. The authors wish to express their gratitude to Professor Giddings for providing a preprint of Ref. *7*, contributing other information which made the comparison with experimental data possible, and giving helpful comments on the manuscript.

Note Added in Proof. A theoretical analysis of the hollow fiber systems used in Ref. *11* may be found in Ref. *27*. While the present article was in press, a similar development was reported in Ref. *28* in the context of ultrafiltration-induced polarization chromatography.

REFERENCES

1. J. C. Giddings, *Sep. Sci.*, *1*, 123 (1966).
2. M. E. Hovingh, G. H. Thompson, and J. C. Giddings, *Anal. Chem.*, *42*, 195 (1970).
3. J. C. Giddings, L. K. Smith, and M. N. Myers, *Ibid.*, *47*, 2389 (1975).
4. J. C. Giddings, Y. H. Yoon, and M. N. Myers, *Ibid.*, *47*, 126 (1975).
5. M. N. Myers, K. D. Caldwell, and J. C. Giddings, *Sep. Sci.*, *9*, 47 (1974).

6. K. D. Caldwell, L. F. Kesner, M. N. Myers, and J. C. Giddings, *Science*, *176*, 296 (1972).
7. L. F. Kesner, K. D. Caldwell, M. N. Myers, and J. C. Giddings, *Anal, Chem.*, *48*, 1834 (1976).
8. J. C. Giddings, F. J. F. Yang, and M. N. Myers, *Anal. Chem.*, *46*, 1917 (1974).
9. J. C. Giddings, F. J. F. Yang, and M. N. Myers, *Sep. Sci.*, *10*, 133 (1975).
10. J. C. Giddings, F. J. F. Yang, and M. N. Myers, *Anal. Chem.*, *48*, 1126 (1976).
11. H. L. Lee, J. F. G. Reis, J. Dohner, and E. N. Lightfoot, *AIChE J.*, *20*, 776 (1974).
12. J. F. G. Reis and E. N. Lightfoot, *Ibid.*, *22*, 779 (1976).
13. J. C. Giddings, M. E. Hovingh, and G. H. Thompson, *J. Phys. Chem.*, *74*, 4291 (1970).
14. J. C. Giddings, *J. Chem. Phys.*, *49*, 81 (1968).
15. J. C. Giddings, *Sep. Sci.*, *8*, 567 (1973).
16. J. C. Giddings, Y. H. Yoon, K. D. Caldwell, M. N. Myers, and M. E. Hovingh, *Ibid.*, *10*, 447 (1975).
17. J. C. Giddings, *Dynamics of Chromatography*, *Part I*, Dekker, New York, 1965.
18. G. I. Taylor, *Proc. R. Soc. London, Ser. A*, *219*, 186 (1953).
19. G. I. Taylor, *Ibid., Ser. A*, *223*, 446 (1954).
20. W. N. Gill and R. Sankarasubramanian, *Ibid., Ser. A*, *316*, 341 (1970).
21. W. N. Gill and R. Sankarasubramanian, *Ibid., Ser. A*, *322*, 101 (1971).
22. R. Aris, *Ibid., Ser. A*, *235*, 67 (1956).
23. S. Krishnamurthy, M. S. Thesis in Chemical Engineering, Clarkson College of Technology, 1976.
24. R. S. Subramanian, *J. Chromatogr.*, *101*, 253 (1974).
25. H. Hsieh, M. S. Thesis in Chemical Engineering, Clarkson College of Technology, 1971.
26. L. F. Kesner, Ph. D. Thesis in Chemistry, University of Utah, 1974.
27. M. R. Doshi, W. N. Gill, and R. S. Subramanian, *Chem. Eng. Sci.*, *30*, 1467 (1976).
28. H. L. Lee and E. N. Lightfoot, *Sep. Sci.*, *11*, 417 (1976).

Received by editor September 13, 1976